Pol. J. Environ. Stud. Vol. 32, No. 3 (2023), 2775-2785
DOI: *10.15244/pjoes/161382* ONLINE PUBLICATION DATE: 2023-04-24

Original Research

Spatio-Temporal Characteristics of Extreme Cold Events and Their Impacts on Population and Economy in Tianjin Binhai New Area, China

Fanchao Meng[1], He Huang[1]*, Jun Guo[1], Guoyu Ren[2, 3], Jialin Zhang[4]

[1]Tianjin Climate Center, Tianjin 300074, China
[2]National Climate Center, China Meteorological Administration, Beijing 10081, China
[3]Department of Atmospheric Science, School of Environmental Studies, China University of Geosciences, Wuhan 430074, China
[4]Tianjin Jinnan District Meteorological Bureau, Tianjin 300350, China

Received: 2 August 2022
Accepted: 17 February 2023

Abstract

Extreme weather events, such as extreme cold events (ECEs), are occurring more frequently due to climate change and variability. The ECEs have severe impacts on people's lives and the economy. In this study, we used observational data for the period 1978-2020 from three national meteorological stations and forty-nine automatic weather stations located in the Tianjin Binhai New Area (TBNA), China, to analyze the spatio-temporal characteristics of ECEs and evaluate their impacts on population and economy. Our results indicate that the annual extreme minimum temperature showed a slight upward trend in the TBNA during the past 43 years. Extreme minimum temperatures were higher in the central part (–15 to –19ºC) and lower in the northern and southern parts of the TBNA (–19 to –23ºC). The cumulative decreases in temperature were higher in the west and lower in the east. ECEs were most frequent in autumn, followed by winter, and least frequent in summer. The months with the most ECEs were October and November. The ECEs lasted longer in the southern part of the TBNA and were shorter in the central and northern parts. The ECEs lasted, on average, approximately 15 days in the south and 7–10 days in most other areas. Places in the TBNA at a high risk of experiencing the ECEs include Gulin subdistrict and other areas in the central part of the TBNA, whereas Zhongtang town and other places in the southern TBNA are low-risk areas. In terms of the impact of ECEs on populations, the central parts of the TBNA such as Hangzhou subdistrict and the northern parts of the TBNA such as Hangu subdistrict are areas of moderate risk; most others are low-risk areas. In terms of the impact of ECEs on Gross Domestic Product (GDP), central parts of the TBNA such as Hujiayuan subdistrict are moderate-risk areas while most others are low-risk areas. Our findings serve as a basis

*e-mail: huanghe09082022@163.com

for decision-making and provide a reference for local governments to mitigate the negative impacts of ECEs.

Keywords: extreme cold events, disaster-causing factors, risk assessment, population and economy, Tianjin Binhai New Area

Introduction

The Sixth Assessment Report of the Intergovernmental Panel on Climate Change stated that climate change caused by human activity is already affecting every region on Earth, causing increases in extreme climate and weather events observed worldwide. Changes in the frequency and intensity of extreme events are exacerbated with every additional increment of global warming [1]. Extreme weather or climate events often lead to different degrees of meteorological disasters [2-3]. As a result, extreme weather and climate events, such as extreme temperatures, are receiving more attention from researchers [4-7]. The greatest impacts of climate change may be attributed to changes in extreme climates, therefore, it becomes very important to analyze extreme climates [8-9].

Extreme cold events (ECEs) are one of the most common weather disasters in north China. Since 2006, winter temperatures have dropped slightly in most parts of this region and ECEs, such as cold waves, have increased significantly [10]. In January 2016, a record-breaking extreme cold event occurred in east China [11-12].I n January 2018, 108 counties and cities in China experienced another extreme cold event, when 4 counties and cities experienced record-breaking minimum temperatures [11]. At the end of 2020 and the beginning of 2021, extreme low-temperature events related to Arctic warming and La Niña swept across mainland China, resulting in record-breaking winter weather in 58 cities [13].

ECEs are weather processes in which cold air accumulates in a source region before moving southward due to circulation [14]. ECEs, such as cold wave, usually lead to severe cooling and windy weather, and are sometimes accompanied by rain, snow and frost [15]. Studies showed that despite overall winter warming in North America, ECEs have increased [16]. The frequency and intensity of cold waves in China decreased between the 1950s and 1980s [17-18]. However, despite global warming, the intensity of cold waves in East Asia has not decreased and the probability of extreme cold waves has increased. Ma et al. [6] found that extreme cold waves in East Asia became more frequent and serious between 1988 and 2016, indicating that the variation inside the atmosphere may be responsible for this phenomenon. Research in China produced similar conclusions. From a study on the Circum-Bohai-Sea region, Duan et al. [19] found that extreme cold wave events have not decreased as climate warming increased. Ma et al. [20] pointed out that the frequency and intensity of cold-air events did not decrease significantly in the Beijing-Tianjin-Hebei region from 1981 to 2015. In Henan Province, study reported that the frequency of cold waves increased significantly since 2011 [21]. Disaster weather caused by ECEs – such as extreme cold, strong winds, and snowstorm-harm human health and agricultural and livestock production and can cause great losses by impacting transportation and interrupting power and communication systems due to freezing roads and wires [22-24]. As a result, risk assessments of disasters caused by ECEs should be conducted.

Although many studies have been conducted on low-temperature events in China, previous studies tended to focus on winter cold waves, with less research on generalized ECEs. Tianjin Binhai New Area (TBNA) located in the lower reaches of the Haihe River Basin, and the Tianjin Port here is the largest comprehensive port in northern China. In recent years, ECEs have occurred frequently in this region, and which is a representative coastal region to study ECEs and its impact on society in China. What are the variation characteristics of the ECEs in recent years in this region? How has the ECEs affected the population and economy in this region? The results of these problems remain unreported. In this study, we analyzed the spatio-temporal characteristics of ECEs and established a disaster risk classification system to assess the impacts of ECEs on the population and economy in the TBNA. Using ArcGIS mapping technology, we showed maps of ECEs disaster risk for population and economy at the township and subdistrict levels. The results of this study could show a further understanding of the change characteristics of ECEs and provide a scientific basis for government to make decisions on concerning low-temperature disaster prevention.

Materials and Methods

Study Area and Data

The TBNA is on the northern part of the North China Plain (38°40′-39°00′N, 117°20′-118°09′E), bordered by the Liaodong Peninsula to the north and the Shandong Peninsula to the south; it is close to Bohai Bay, where the Hai River flows into the sea. The coastline is 153 km long and the TBNA is also the eastern starting point of the Eurasian Land Bridge, providing an important gateway to the sea between the capital, Beijing, and the northwestern and northern regions of the country. The total area of the TBNA is 350 km^2; it comprises the three administrative districts of Hangu, Tanggu,

and Dagang, and nineteen towns or subdistricts. The area has a typical warm temperate semi-humid and semi-arid monsoon climate, with four distinct seasons.

In this study, the daily surface air temperature data were obtained from national meteorological stations in the Hangu, Tanggu, and Dagang, including daily minimum temperature and daily mean temperature data from 1978 to 2020, and the hourly mean temperature data from 49 automatic weather stations. These data have undergone a strict quality control to ensure their reliability and accuracy. The scale of the basic geographic information, mainly in terms of administrative (district, township, and subdistrict) boundaries, is greater than 1:100,000. The locations of the study area and weather stations are shown in Fig. 1.

Definition of Extreme Cold Event

Based on the QX/T 393-2017 standard of monitoring indices of cold air processes, whereby an extreme cold event is judged as cold air above moderate intensity (the drop of daily minimum temperature in 48 hours ≥6ºC) at a single meteorological station lasting for two or more days. The first and last days that satisfy the extreme cold event conditions are the start and end dates thereof.

Selection and Treatment of Disaster-Causing Factors

In this study, the disaster-causing factors include the maximum of the drop of minimum temperature of the process ($MaxΔT_{min}$), the cumulative of the drop of minimum temperature of the process ($CumΔT_{min}$), the minimum temperature of the process ($MinT_{min}$), the average minimum temperature of the process ($AveT_{min}$), and the duration of the process (D_{cold}).

We normalized and transformed dimensional disaster-causing factor values into nondimensional values to eliminate the dimensional difference of each indicator. For the normalization method, we used linear function normalization, and the equation is as follows:

$$X' = \frac{x - x_{\min}}{x_{\max} - x_{\min}} \tag{1}$$

where x' is the normalized value, x is the sample data, x_{min} is the minimum value in the sample data, and x_{max} is the maximum value in the sample data.

Risk Assessment of ECEs

The equation for calculating the risk index of disaster-causing factor is as follows:

$$H = A \times MaxΔT_{\min} + B \times CumΔT_{\min} + C \times MinT_{\min} + D \times AveT_{\min} + E \times D_{cold} + F \times AOF \tag{2}$$

where H is the risk index of disaster-causing factor, AOF is the annual occurrence frequency of ECEs. A, B, C, D, E, and F are the weight coefficients. $MaxΔT_{min}$, $CumΔT_{min}$, $MinT_{min}$, $AveT_{min}$, D_{cold}, and AOF are normalized disaster-causing factor indexes.

In this study, the information entropy weighting method can be used to determine the weight coefficient in the risk assessment of ECEs. The higher the degree of order in a system, the higher the entropy value and lower the weight; conversely, the higher the degree of disorder in a system, the lower the entropy value and higher the weight. Assuming that the evaluation system is composed of m indicators and n objects, we first calculate the indicator specific weight P_{ij} of indicator value r_{ij} of the jth object under the ith indicator:

$$P_{ij} = \frac{r_{ij}}{\sum_{i=1}^{n} r_{ij}} \quad (i = 1,2\cdots\cdots, m; j = 1,2\cdots\cdots, n) \tag{3}$$

The entropy value S_i of the ith indicator is calculated as follows:

$$S_i = -\frac{1}{\ln n}\sum_{j=1}^{n} P_{ij} \ln P_{ij} \quad (i = 1,2\cdots\cdots, m; j = 1,2\cdots\cdots, n) \tag{4}$$

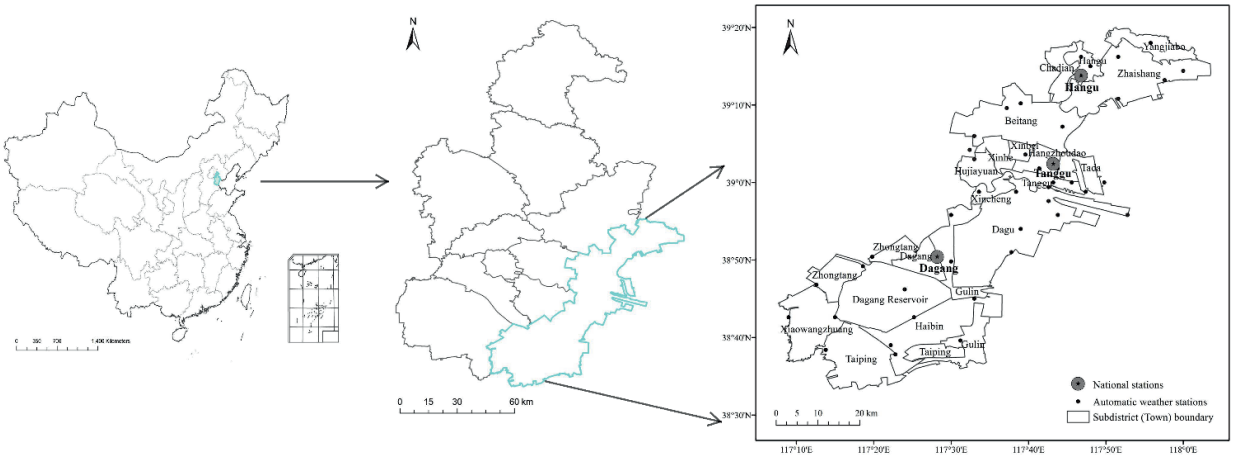

Fig. 1. Locations of weather stations in the Tianjin Binhai New Area (TBNA).

The entropy weight of the *i*th indicator is calculated next and the objective weight of the indicator W_i is determined as below:

$$W_i = \frac{1-S_i}{\sum_{i=1}^{m}(1-S_i)}(i = 1,2\cdots\cdots,m) \quad (5)$$

Based on the distribution of the risk index of disaster-causing factor values, we divided risk into four levels: extremely high risk (I level), highrisk (II level), moderaterisk (III level), and low risk (IV level). We then drew a risk index distribution map.

Exposure Assessment of Hazard-Bearing Body

In this study, exposure assessment involved standardizing the total population density and gross domestic product (GDP) of each township or subdistrict in the TBNA as indicators with which to evaluate exposure to ECEs. For example, we used the ratio of the population to their total area of each township or subdistrict in the TBNA as an exposure index of hazard-bearing body. The method of calculating the exposure index is as follows:

$$E = \frac{S_E}{S} \quad (6)$$

Where E is the exposure index of the hazard-bearing body (population), S_E is the total population of township or subdistrict, and S is the total area of each township or subdistrict. Equation (1) is used to normalize the exposure index to obtain the final exposure index of the hazard-bearing body.

Vulnerability Assessment of Hazard-Bearing Body

We only conducted the extreme cold disaster vulnerability assessment for the population. The proportion of the population under 14 and over 65 years of age in the townships or subdistricts of the TBNA as an index of vulnerability (population) for ECEs after standardization. The specific calculation method is as follows:

$$V = \frac{S_v}{S} \quad (7)$$

where V is the vulnerability index of the hazard-bearing body (population), S_v is the population under 14 and above 65 years of age of township or subdistrict, and S is the total population of township or subdistrict. We normalized the population vulnerability index according to Equation (1) to obtain the final population vulnerability index.

Comprehensive Risk Assessment and Zoning of Extreme Cold Disaster

Generally, the risk of extreme cold disasters depends on a combination of three factors: the risk of disaster-causing factors, exposure of the hazard-bearing body, and vulnerability of hazard-bearing body. Extreme cold disaster risk zoning is comprehensive consideration of division of spatial units based on the results of risk assessment for different hazard-bearing body and administrative divisions.

The method of calculating the risk assessment index of extreme cold disaster for disaster-bearing body is as follows:

$$R = \mathrm{H} \times \mathrm{E} \times \mathrm{V} \quad (8)$$

where R is the risk assessment index of extreme cold disaster for disaster-bearing body, H is the risk index of disaster-causing factor, E is the exposure index of the hazard-bearing body, V is the vulnerability index of the hazard-bearing body.

In this study, standard deviation method was used to divide the comprehensive risk of extreme cold disaster into five levels (Table 1).

Results

Spatio-Temporal Characteristics of Related Disaster-Causing Factors

Extreme Minimum Temperature

Between 1978 and 2020, the annual extreme minimum temperature showed increased trend at 3 national meteorological stations, and the upward trend at Dagang station was the most notable. The extreme minimum temperature at Hangu station was the lowest in 2010 (–22.5ºC) and highest in 2015 (–10.6ºC). At Tanggu station, it was lowest in 2010 (–18.4ºC) and highest in 1989 (–8.5ºC). At Dagang station, the extreme minimum temperature was lowest in 1990 (–19.4ºC) and highest in 2017 (–8.6ºC) (Fig. 2).

Table 1. The classification standard of comprehensive risk assessment of extreme cold disaster.

levels	The classification standard
Highest	R≥ave + σ
Higher	ave + 0.5σ≤R<ave + σ
Moderate	ave – 0.5σ≤R<ave + 0.5σ
Lower	ave – σ≤R<ave – 0.5σ
Lowest	R<ave – σ

Note: ave is the mean value of non-zero risk assessment value, σ is the standard deviation of non-zero risk assessment value.

The lowest monthly extreme minimum temperatures at Tanggu, Hangu, and Dagang stations all occurred in January: –22.5ºC at Hangu station on January 6, 2010; –18.4ºC at Tanggu station on January 6, 2010; and –19.4ºC at Dagang station on January 31, 1990 (Fig. 3).

The spatial distribution of extreme minimum temperatures of ECEs in the TBNA could be characterized as high in the central part (–15 to –19ºC, in Tanggu station) and low in the northern and southern parts (–19 to –23°C in Hangu station) in the north and Dagang station in the south) of the TBNA (Fig. 4).

The Drop of Minimum Temperature of ECEs

Of the decreases in the maximum of the drop of minimum temperature of the process ($MaxΔT_{min}$) between 1978 and 2020, the largest decrease at Hangu station was 11.1ºC, where the annual average was 5.0ºC; the largest at Tanggu station was 13.0°C, with an annual average of 5.2ºC; and the largest at Dagang station was 12.2ºC, with an annual average of 5.1ºC (Fig. 5).

In terms of the cumulative of the drop of minimum temperature of the process ($CumΔT_{min}$), the overall spatial distribution in the TBNA could be characterized as higher in the west and lower in the east. The $CumΔT_{min}$ decreases in western Beitang subdistrict in the central part of the TBNA and western New town were approximately 14ºC; in the Hangu and Chadian subdistricts and Yangjiabo town in the northern part of the TBNA, approximately 10°C; and in most other parts of the TBNA, they were 11–13ºC (Fig. 6).

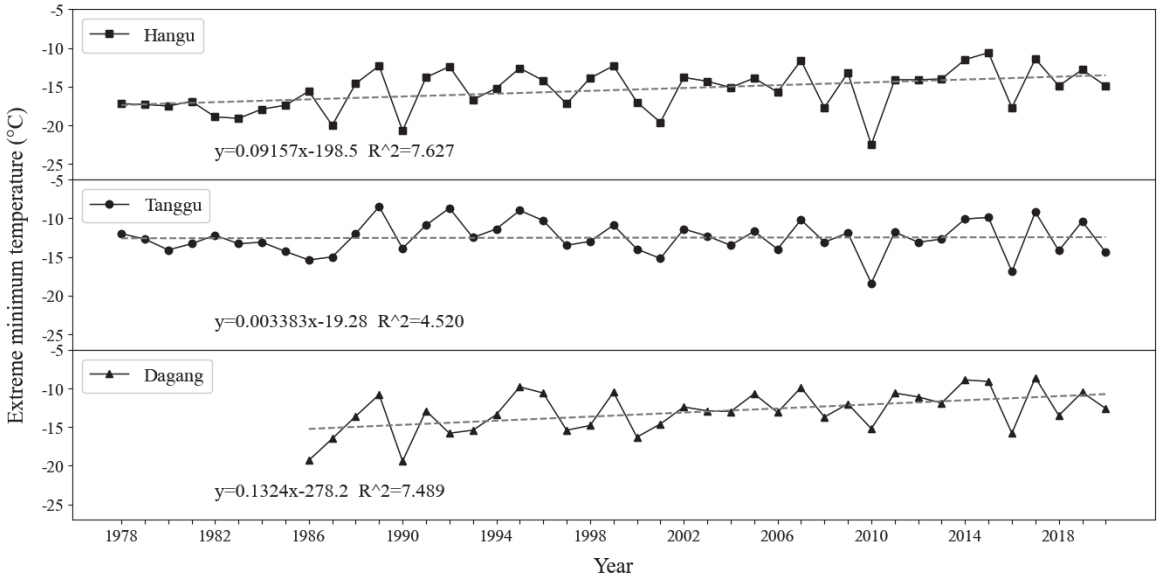

Fig. 2. Changes in annual extreme minimum temperatures atthe three stations of the TBNA during 1978-2020.

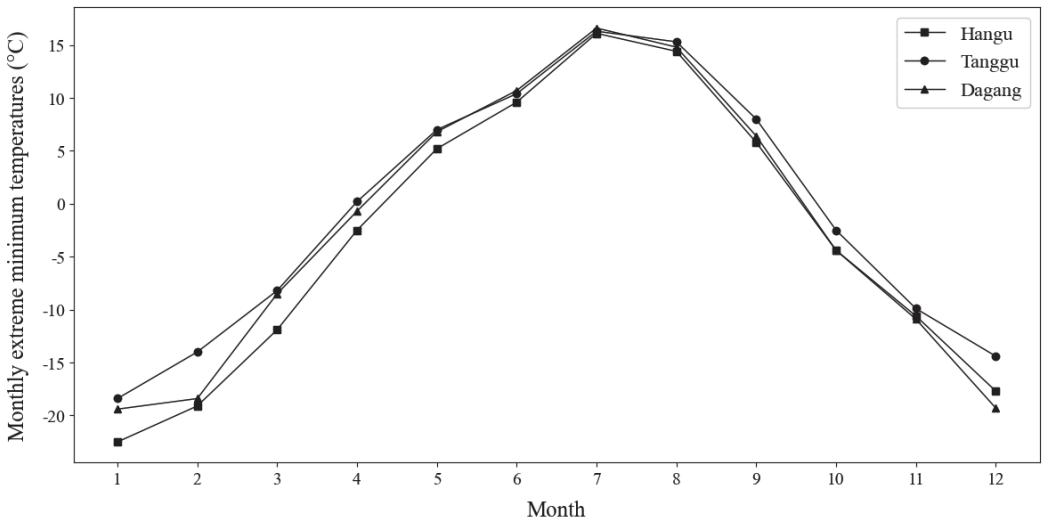

Fig. 3. Monthly extreme minimum temperatures at the three stations of the TBNA during 1978-2020.

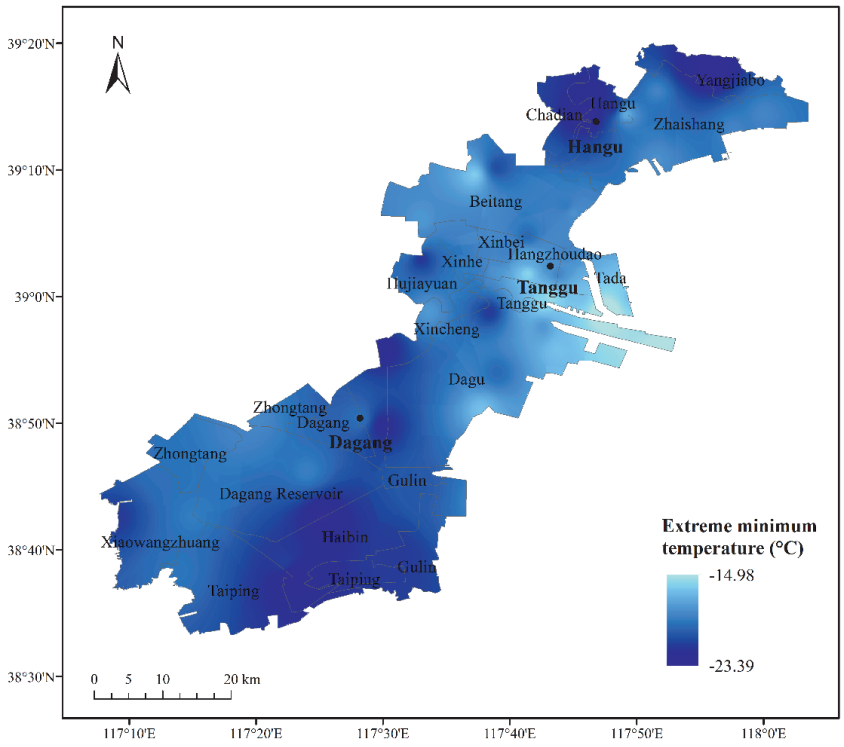

Fig. 4. Spatial distribution of extreme minimum temperature of the TBNA during 1978-2020.

Frequency of ECEs

At Hangu station, 219 ECEs occurred between 1978 and 2020, averaging 5.1 events per year. The most frequent of ECEs (9 times) occurred in 1981 and 2007 and least frequent (1 times) in 2001 and 2006. A total of 191 ECEs occurred at Tanggu station, averaging 4.4 per year. The ECEs were the most frequent in 1999 and 2018 (8 times) and least frequent in 2001 and 2014 (1 times). A total of 161 ECEs occurred at Dagang station, averaging 4.6 per year. They were most frequent in 1988 (8 times) and least frequent in 2013 and 2014 (1 times; Fig. 7).

In terms of the monthly distribution of the ECEs (Fig. 8), the ECEs were most frequent in autumn (September to November), with an average of 97 at the three stations in the TBNA; followed by winter (December to February), with an average of 47 occurrences, and then summer (June to August) with an average of 14 occurrences. The months with the most ECEs throughout the year were October and November, and the month with the fewest was July.

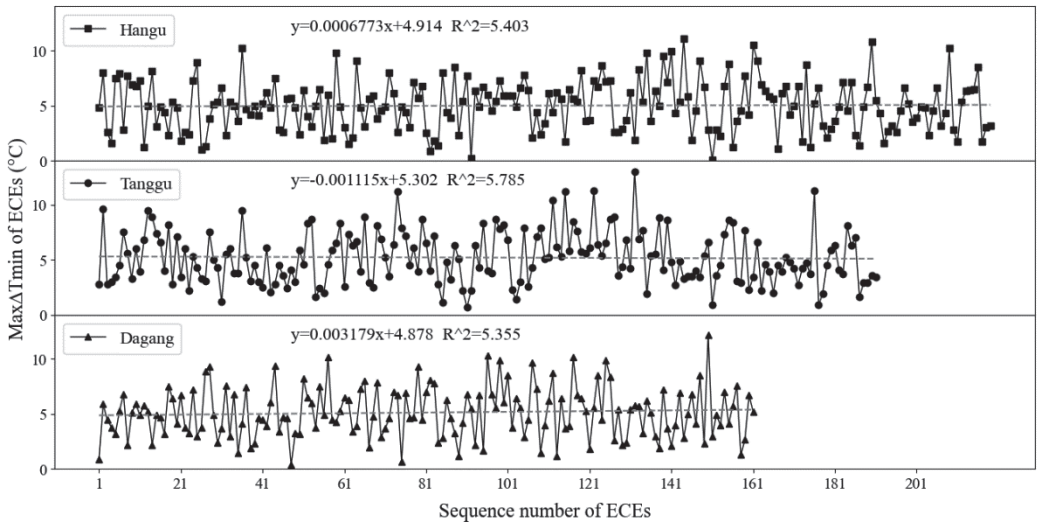

Fig. 5. The MaxΔT_{min} of ECEs at the three stations of the TBNA during 1978-2020.

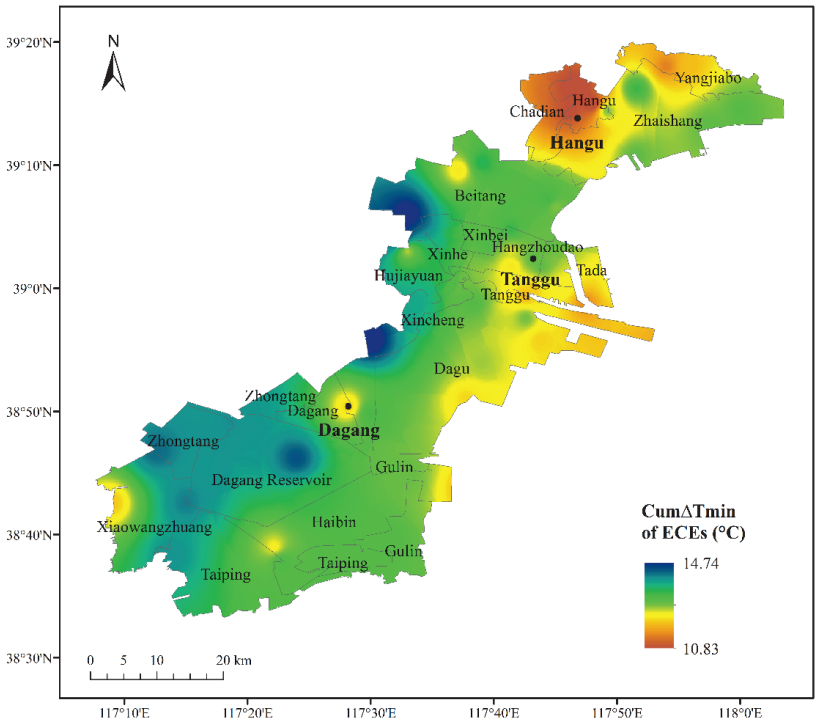

Fig. 6. Spatial distributionof the$CumΔT_{min}$of ECEs of the TBNA during 1978-2020.

Duration of ECEs

The duration of ECEs in the TBNA could be spatially characterized as longer in the southern and shorter in the central and northern regions. The duration of ECEs in places such as Haibin subdistrict and Taiping town in the south and Xiaowangzhuang town in the southwest of the TBNA was approximately 15 days. In most other areas of the TBNA, the average duration was approximately 7-10 days (Fig. 9).

Risk Assessment of ECEs

Considering the spatial distribution of risk classification of ECEs in the TBNA, areas at extremely high risk (I level) include Gulin subdistrict in the central region; high risk areas (II level) include Dagu subdistrict, Chadian subdistrict, and Haibin subdistrict in the central, northern, and southern regions, respectively; moderate risk areas (III level) include Dagang subdistrict in the south and Hujiayuan subdistrict in the north; and low risk areas (IV level)

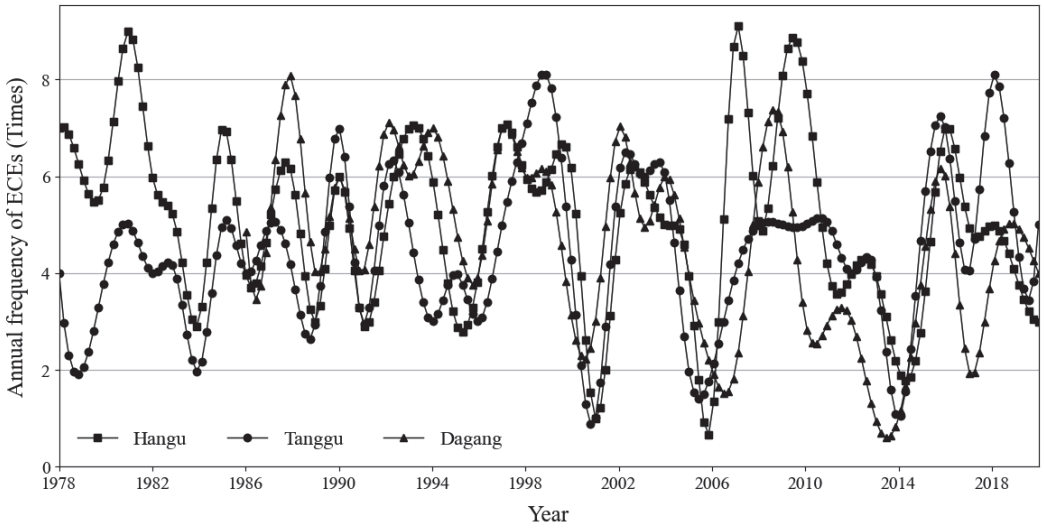

Fig. 7. Time series of the annual frequency of ECEs at the three stations of the TBNA during 1978-2020.

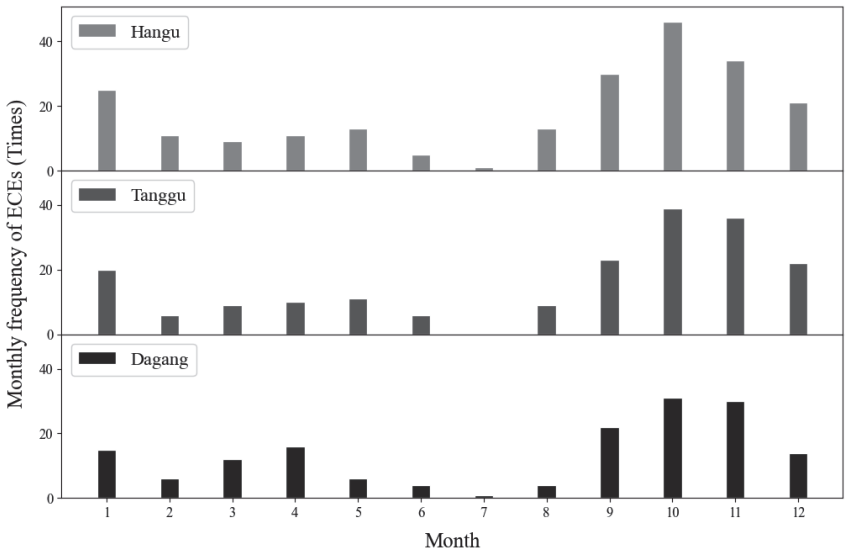

Fig. 8. Monthly frequency of ECEs at the three stations of the TBNA during 1978-2020.

include Zhongtang town in the south and Zhaishang subdistrict in the north (Fig. 10).

Risk Zoning of ECEs for Different Hazard-Bearing Body (Population and GDP)

In terms of risk zoning of ECEs for population of the TBNA during 1978-2020, the areas at moderate risk are Hangzhou and Xinbei subdistricts and Xincheng town in the central part of the TBNA; Xiaowangzhuang and Taiping town and Haibin subdistrict in the south; and Hangu subdistrict in the north. Most of the remaining areas are at lower risk level (Fig. 11 a). In terms of risk zoning of ECEs for GDP, the areas at moderate risk are the Hujiayuan, Xinhe, Xinbei, Hangzhoudao, Taida, and Tanggu subdistricts in the central of TBNA, as well as Hangu subdistrict in the north and Dagang subdistrict in the south. Most of the remaining areas are at lower risk level (Fig. 11 b).

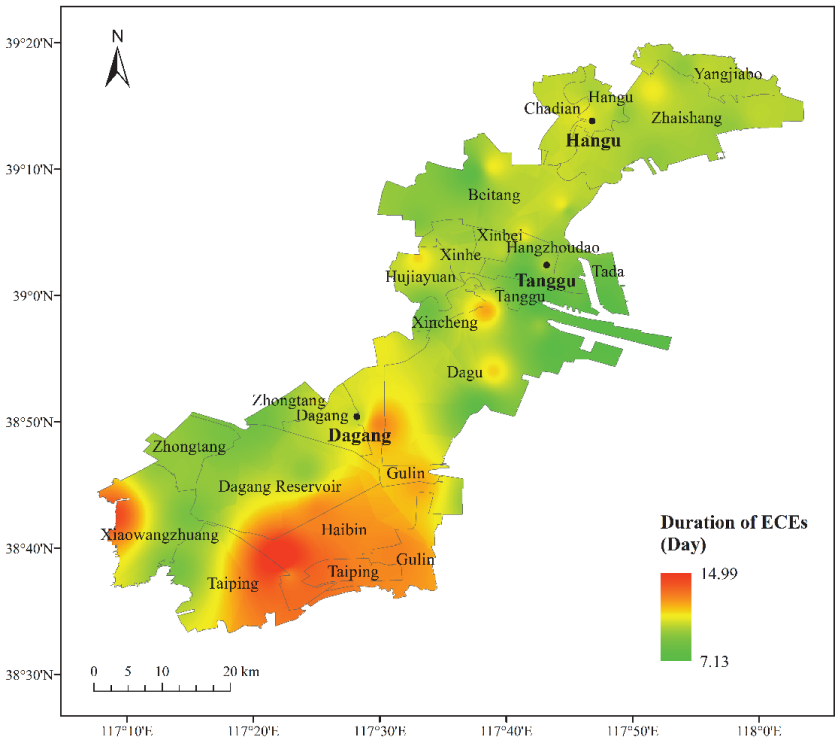

Fig. 9. Spatial distribution of the duration of ECEs of the TBNA during 1978-2020.

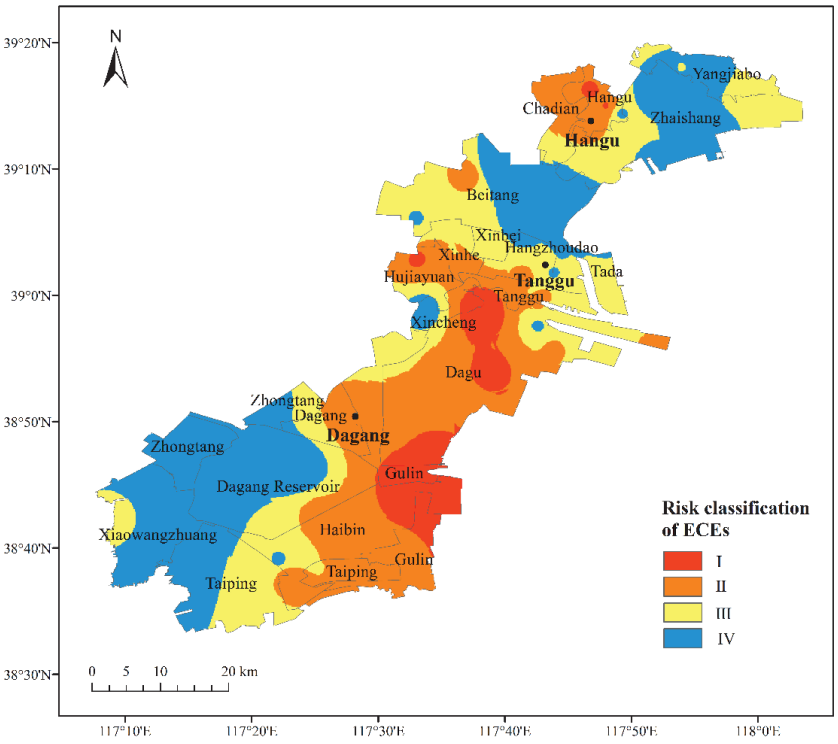

Fig. 10. Spatial distribution of risk classification of ECEs of the TBNA during 1978-2020.

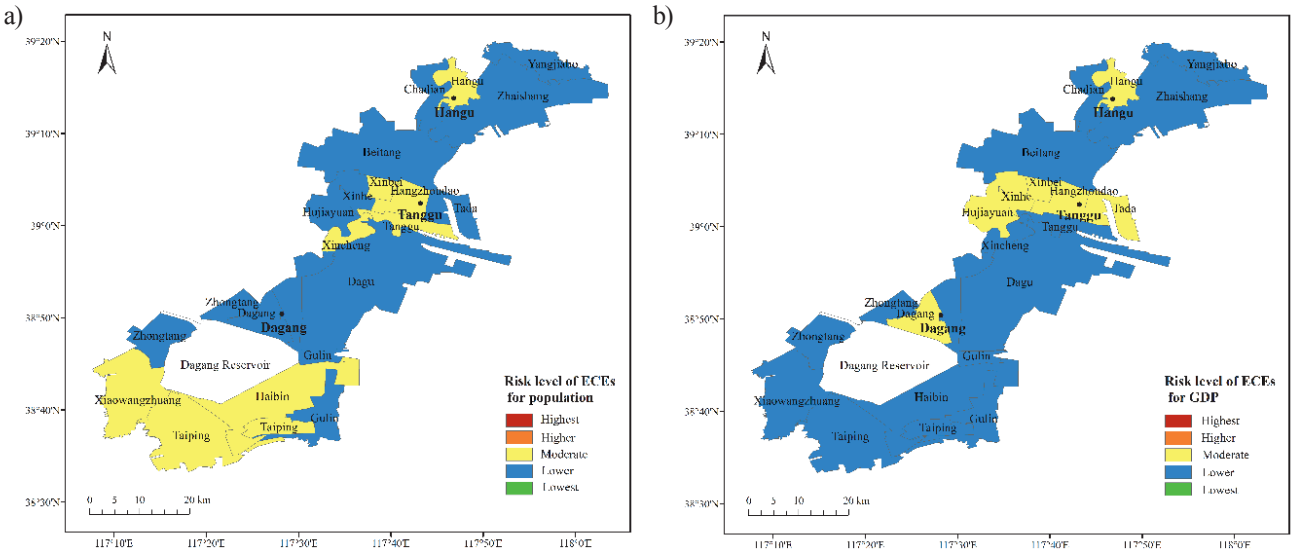

Fig. 11. Risk zoning of ECEs for population and GDP of the TBNA during 1978-2020.

Discussion and Conclusions

In recent decades, climate change and variability caused change in extreme temperature events frequency and intensity, which have been a significant issue around the world [25]. A study on extreme temperature change of the last 110 years in Northeast China suggested that the frequency of cold surge events increased significantly, occurring from the mid-1950s to late-1980s [26]. The extreme low temperatures are closely related to regional warming [27], has exerted a considerable impact on the global ecosystem and economic society [28-29]. Coastal regions are also affected by extreme low temperatures. To understand the variation characteristics of the ECEs and its social impact in coastal regions, we conducted a study in the TBNA, China. In this study, we analyzed the spatio -temporal characteristics of ECEs during a 43-year period (1978-2020) and evaluated the impact of ECEs on population and GDP in this region.

In terms of intensity of ECEs, we found that the annual extreme minimum temperature at 3 national meteorological stations in the TBNA trended upward between 1978 and 2020. The lowest extreme minimum temperature, –22.5ºC, was observed at Hangu station in 2010. Extreme minimum temperatures could be characterized as higher in the central part of the TBNA and lower in the southern and northern parts. The extreme minimum temperature at Tanggu, in the central part of the TBNA, was –15 to –19ºC; at Hangu in the north and Dagang in the south, it was –19 to –23ºC. A study on cold-air events in Xinjiang, China, by Duan et al. [30] showed that the cumulative decreases in temperature during cold-air processes decreased significantly in the Yili Valley over the past 56 years. Here, we found that the cumulative of the drop of minimum temperature of the process ($CumΔT_{min}$) in the TBNA were higher in the west and lower in the east. The $CumΔT_{min}$ in the central and western regions was approximately 14ºC, and in the north it was approximately 10ºC. During the 43 years of the study period, the maximum of the drop of minimum temperature of the process ($MaxΔT_{min)}$, 13.0ºC, was the largest value observed at Tanggu station.

In terms of the frequency and duration of ECEs, we found that ECEs were most frequent in autumn, with an average of 97 occurrences at the three stations in the TBNA, followed by winter; they were the least frequent in summer. The October-November period had the most ECEs throughout the year. Wang et al. [17] found that autumn had the most frequent cold waves. In northern China, cold wave events occurred most active in March and from October to November [15]. Studies of the Circum-Bohai-Sea region show that cold waves occurred most frequently in November, followed by December and January; cold waves occurred less frequently, in September and April [19]. Ma et al. [20] reported similar findings, indicating that in the Beijing-Tianjin–Hebei region, cold-air processes occurred with greatest frequency and intensity in November. Moreover, we also found that in the past 43 years, Hangu station recorded the most cold-air processes, with 219 times, averaging 5.1 times per year. In 1981 and 2007, the cold air activity was the most frequent (9 times each) at Hangu station. Furthermore, the duration of ECEs lasted longer in the southern part of the TBNA and were shorter in the central and northern parts in this study. Duration of ECEs, on average, approximately 15 days in the south and 7-10 days in most other areas.

Extreme low temperature has an important impact on population and social economy. A study indicated that cold waves can increase the all-cause or non-accidental mortality by 10% in general [31]. Due to cold wave and frost damage, the affected area of crops accounted for about 5% of the total affected area in Henan Province, China [21]. Clarifying the spatial and temporal characteristics of ECEs can provide guidance for government to prepare and response to disasters. The disaster risk assessment is the first step in national emergency management. Therefore, we evaluated the impact of ECEs on population and GDP in this study.

The results of the risk assessment of ECEs in this study indicated that areas at extremely high risk (I level) include Gulin subdistrict in the central part of the TBNA; high risk areas (II level) include Dagu subdistrict in the central region and Haibin subdistrict in the south; areas at moderate risk areas (III level) include Dagang subdistrict in the south and Xinhe subdistrict in the north; and low risk areas (IV level) include Zhongtang town in the south. From the perspective of risk zoning of ECEs for population, the Hangzhoudao, Xinbei subdistrict in the central part of the TBNA, and Xiaowangzhuang and Taiping town and Haibin subdistrict in the south are moderate risk areas while most others are lower risk areas. The results of risk zoning of ECEs for GDP showed that the Hujiayuan, Xinhe, Xinbei subdistricts in the central of TBNA, as well as Hangu subdistrict in the north and Dagang subdistrict in the south are moderate-risk areas, while most of the other areas in the TBNA are lower risk level.

Notably, we only analyzed the spatio-temporal characteristics of ECEs and assess its impacts on population and GDP. However, the mechanisms influencing the occurrence and change of ECEs remains to be further explored to deepen understanding of extreme cold climate event. Moreover, due to insufficient data on the disaster-bearing bodies at the present stage, future studies are required to quantitatively assess the impact of ECEs for other disaster-bearing bodies.

Acknowledgments

This work was financially supported by the National Key Research and Development Program (2018YFA0605603), the National Natural Science Foundation of China (42005129).

Conflict of Interest

The authors declare no conflict of interest.

References

1. IPCC. Climate Change 2021, the Physical Science Basis. Contribution of Working Group I to the Sixth Assessment Report of the Intergovernmental Panel on Climate Change. Cambridge University Press: Cambridge, UK, **2021**.
2. CAI M., WEI G. A fuzzy social vulnerability evaluation from the perception of disaster bearers against meteorological disasters. Natural Hazards. **103** (2), 2355, **2020**.
3. LI H., XI W.S., ZHANG L.J., ZANG S.Y. Snow-disaster risk zoning and assessment in Heilongjiang Province. Sustainability. **13** (24), 14010, **2021**.

4. MA J.H., MAO Z.C., YU Z.Q., QU Y.H., GENG F.H., XU J.M., CHEN M. Analysis of the temporal and spatial distribution of haze and its influencing factors in Shanghai. Pol. J. Environ. Stud. **25** (5), 1965, **2016**.
5. WANG G., YAN D.H., HE X.Y., LIU S.H., ZHANG C., XING Z. Q., KAN G.Y., QIN T.L., REN M.L., LI H. Trends in extreme temperature indices in Huang-Huai-Hai River Basin of China during 1961-2014. Theor.Appl. Climatol. **134** (1), 51, **2018**.
6. MA S.M., ZHU C.W. Extreme cold wave over East Asia in January 2016: A possible response to the larger internal atmospheric variability induced by Arctic warming. J. Climate. **32** (4), 1203, **2019**.
7. XU X.M., TANG Q.H. Meteorological disaster frequency at prefecture-level city scale and induced losses in mainland China during 2011-2019. Natural Hazards. **109** (1), 827, **2021**.
8. ZHANG X.B., HEGERL G., ZWIERS F.W., KENYON J. Avoiding in homogeneity in percentile-based indices of temperature extremes. J. Climate. **18** (11), 1641, **2005**.
9. PALANISWAMI S., MUTHIAH K. Change point detection and trend analysis of rainfall and temperature series over the Vellar River basin. Pol. J. Environ. Stud. **27** (4), 1673, **2018**.
10. FU D.X., DING Y.H. The study of changing characteristics of the winter temperature and extreme cold events in China over the past six decades. Int. J. Climatol. **41** (4), 2480, **2021**.
11. QIAN C., ZHANG X.B., LI Z. Linear trends in temperature extremes in China, with an emphasis on non-Gaussian and serially dependent characteristics. Climate dynamics. **53** (1), 533, **2019**.
12. HO H.C., CHAN T.C., XU Z.W., HUANG C.R., LI C.C. Individual- and community-level shifts in mortality patterns during the January 2016 East Asia cold wave associated with a super El Niño event: Empirical evidence in Hong Kong. Sci. Total. Environ. **711**, 135050, **2020**.
13. ZHENG F., YUAN Y., DING Y.H., LI K.X., FANG X.H., ZHAO Y.H., SUN Y., ZHU J., KE Z.J., WANG J., JIA X.L. The 2020/21 extremely cold winter in China influenced by the synergistic effect of La Niña and Warm Arctic. Adv. Atmos. Sci.**39**, 546, **2022**.
14. YU B., LI S., HUANG F.X., XING N., DU J. Comparative analysis of continuous cold wave events in Beijing-Tianjin-Hebei region in January 2016. Journal of Arid Meteorology. **37** (6), 954, **2019** [In Chinese].
15. ZHU Q.G., LIN J.R. SHOU S.W., TANG D.S. Principles and methods of synoptic meteorology. China Meteorological Press: Beijing, China, **2000** [In Chinese]
16. ANANDHI A., HUTCHINSON S., HARRINGTON J., RAHMANI V., KIRKHAM M.B., RICE C.W. Changes in spatial and temporal trends in wet, dry, warm and cold spell length or duration indices in Kansas, USA. Int. J.Climatol. **36** (12), 4085, **2016**.
17. WANG Z.Y., DING Y.H. Climate change of the cold wave frequency of China in the last 53 years and the possible reasons. Chinese Journal of Atmospheric Sciences. **30** (6), 1068, **2006** [In Chinese].
18. ZHANG Z.J., QIAN W.H. Identifying regional prolonged low temperature events in China. Adv. Atmos. Sci. **28** (2), 338, **2011**.
19. DUAN L.Y., LIU A.X., YU L.L. Temporal and spatial distribution of cold wave and its variation around the Bohai Sea region from 1961-2010. Journal of Meteorology and Environment. **29** (4), 54, **2013** [In Chinese].
20. MA N., HE L.Y., LIANG S.J., GUO J. Low-frequency characteristics of winter-time cold air activity in the Beijing-Tianjin-Hebei region and the impacts of low-frequency variation of the Siberian High. Acta Geographica Sinica. **75** (3), 485, **2020** [In Chinese].
21. WANG J.F., ZUO X., ZHU Y.Y. Spatial-temporal distribution of cold wave and its influence on agriculture in Henan province during 1961-2019. Meteorological and Environmental Sciences. **44** (4), 8, **2021** [In Chinese].
22. DING Z., LI L.J., WEI R.Q., DONG W.Y., GUO P., YANG S.Y., LIU J., ZHANG Q.Y. Association of cold temperature and mortality and effect modification in the subtropical plateau monsoon climate of Yuxi, China. Environ. Res. **150**, 431, **2016**.
23. XIE Z.W., BLACK R.X., DENG Y. Planetary and synoptic-scale dynamic control of extreme cold wave patterns over the United States. Climate Dynamics. **53** (3), 1477, **2019**.
24. MALIK P., BHARDWAJ P., SINGH O. Distribution of cold wave mortalities over India: 1978-2014. Int. J.Disast. Risk Re. **51**, 101841, **2020**.
25. FERRELLI F., BRENDEL A.S., PERILLO G.M.E., PICCOLO M.C. Warming signals emerging from the analysis of daily changes in extreme temperature events over Pampas (Argentina). Environ. EarthSci. **80** (12), 1, **2021**.
26. YU X.J., REN G.Y., ZHANG P.F., HU J.B., LIU N, LI J.P., ZHANG C.C. Extreme temperature change of the last 110 years in Changchun, Northeast China. Adv. Atmos. Sci.**37** (4), 347, **2020**.
27. TONG S.Q., LI X.Q., ZHANG J.Q., BAO Y.H., BAO Y.B., NA L., SI A. Spatial and temporal variability in extreme temperature and precipitation events in Inner Mongolia (China) during 1960-2017. Sci. Total. Environ. **649**, 75, **2019**.
28. LIM E.P., HENDON H.H., SHI L., DE BURGH-DAY C., HUDSON D., KING A., TREWIN B., GRIFTHS M., MARSHALL A. Tropical forcing of Australian extreme low minimum temperatures in September 2019. Climate Dynamics. **56** (11), 3625, **2021**.
29. SHI G.X., YE P. Assessment on temporal and spatial variation analysis of extreme temperature indices: a case study of the Yangtze River Basin. Int. J. Environ. Res. Public Health. **18** (20), 10936, **2021**.
30. DUAN J.Z., MAO W.Y., HUANG Y.J., JIANG Y.A., LI H.Y. Climate change characteristics of cold air process in the Yili Valley in recent 56 years. Journal of Arid Meteorology. **36** (5), 758, **2018** [In Chinese].
31. RYTI N.R., GUO Y., JAAKKOLA J.J. Global association of cold spells and adverse health effects: a systematic review and meta-analysis. Environ. Health Perspect. **124** (1), 12, **2016**.